Fully Digital Amplitude Estimation System for In-Vivo Stem Impedance Monitoring

Fully Digital Amplitude Estimation System for In-Vivo Stem Impedance Monitoring

Stefano Calvo*, Danilo Demarchi*, and Umberto Garlando*
*Department of Electronics and Telecommunications, Politecnico di Torino, Torino, Italy
Email: stefano.calvo@polito.it

***Abstract*—Smart agriculture aims to improve food production and reduce the waste of water and chemicals by monitoring the crops with sensors. Direct and in-vivo crop monitoring can improve the information extracted and increase the impact of smart agriculture. Here, we propose a system to estimate the amplitude of a signal traveling inside a plant stem in vivo. The amplitude of this signal is strictly related to the impedance of the plant, a promising parameter to monitor plant status. This approach allows monitoring the plant impedance with an electric signal carrying other information. The plant stem will act as a communication channel, removing the need for wireless communication systems.**

***Index Terms*—Smart Agriculture, water stress, in-vivo monitoring, stem electrical impedance, plant's resilience**

I. Introduction

World population growth and climate change represent two significant threats to food security [1], [2]. Recent studies state that the world population is expected to reach 10 billion by the end of the 21st century [1]. This dramatic population increase implies that food production must be boosted to keep up with this growth. These two processes feed a vicious circle: the higher the global demand for food, the higher its environmental impact. Nowadays, food production is responsible for more than 25% of the total greenhouse gas emissions worldwide and more than 70% of the total freshwater withdrawals [3], and this impact is destined to increase. Because of these issues, food security is severely threatened. Tackling this problem is one of the main goals of Smart Agriculture. This research field aims to merge farming and engineering knowledge to increase field yields and reduce environmental impact simultaneously. Smart agriculture's most common approach is to monitor the environment surrounding the crops [4], [5]. This approach provides valuable information that may help farmers improve crops' health status. Nevertheless, it does not take into account the plant itself. In a recent study, authors highlighted that plants can suffer despite the fact that the environment surrounding them does not pose any threat to their health [6]. Behaviors such as this suggested that directly monitoring the plant rather than its surroundings may lead to more meaningful information instead of merely focusing on the environmental analysis [6], [7]. One of the most promising parameters that could be exploited to directly monitor plants in-vivo and real-time is the stem (or trunk) electrical impedance [6], [8], [9]. This parameter showed that it could be used to derive information relative to plants' water stress status [10], [11]. It is strictly related to the soil water potential (SWP). This quantity is a reliable and widely used indicator of crop watering stress status since it measures a plant's effort to absorb water from the soil[12], [13]. Therefore, it takes into account both soil water content and texture. In-vivo and real-time impedance analysis proved to be useful in assessing valuable information not only relative to the plants' health status but also to the fruit ripening stage [14], [15]. This work presents a novel approach to reading plants' in-vivo stem electrical impedance. Our methodology exploits plants' trunks' conductive (and thus resistive) behavior [16]–[18], and it relies on the evaluation of an electrical signal attenuation that traveled inside the stem (further details are given in the section II). The measurements described in this work involved a *Nicotiana Tabacum* plant growing in its pot and around $60\,\mathrm{cm}$ tall. This plant species is easy to grow and can adapt to indoor conditions. Therefore, it has been chosen.

The paper is organized as follows. In section II, the devices designed to implement the presented methodology are detailed. In section III, data collected with the presented method are shown, and they are discussed. Finally, section IV sums up the work done and draws the relative conclusions.

II. Experimental Set-Up

This work presents a novel methodology and the related system to inspect in-vivo stem electrical impedance. Differently from previous works [6], [8], [9] where only a portion of the stem was considered, here the whole stem was monitored. This feature is achieved by exploiting an electric signal's attenuation while traveling through a resistive medium. Analyzing the impedance of the whole stem instead of focusing on a small portion may provide more accurate information regarding the overall plant's stress status. The developed system comprises two devices: a transmitter and a receiver. These two devices are entirely independent of one another. Therefore, they did not share the voltage reference (GND). The system setup and the path followed by the signal are depicted in figure 1. The transmitter's goal was to inject the signal into the plant. The receiver's was to read this signal and transmit its characteristics to a laptop, where data analysis was carried out. The transmitter will be described first. Then, the receiver will be detailed.

979-8-3503-8122-1/24/$31.00 ©2024 IEEE

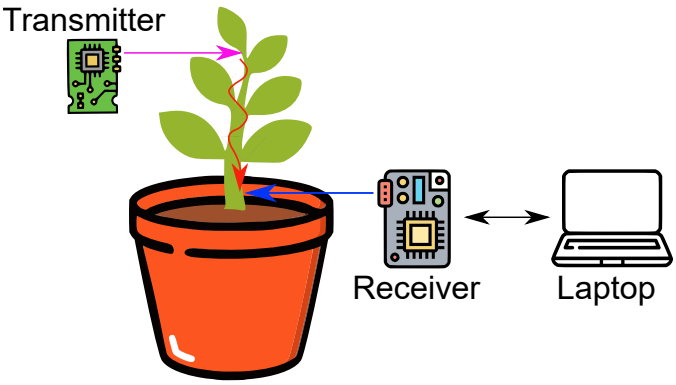

Fig. 1. System developed to monitor the stem electrical impedance. The red wavy arrow highlights the signal's path to travel from the transmitter to the receiver. The black arrow is the cabled connection that connects the receiver to a laptop where data are stored. The signal traveled along the whole plant stem for approximately equal to 40 cm.

A. Transmitter

As stated, this device aimed to inject the signal inside the plant. Since the modulation exploited to monitor the impedance was an amplitude one, injecting a signal with a fixed peak-to-peak amplitude was crucial. Moreover, since the system is meant to be deployed in the fields, the device's complexity and cost must be kept as low as possible. Therefore, a simple ring oscillator (RO) constituted the transmitter. The RO was a 74HC04 by Diodes Inc. connected to have five inverters and a capacitor in a loop, generating a square wave with a frequency equal to 80 kHz. The sixth available inverter in the integrated circuit was exploited as a driver to inject the signal into the plant and an impedance decoupler. This was necessary to disentangle the signal's amplitude and frequency from the plant stem impedance, improving signal stability over time. This feature is critical in this application, and the reason will be clarified in section II-B. The ring oscillator schematic is depicted in figure 2. The signal injection and collection were performed by piercing the plant with a 0.4 mm stainless steel needle connected to the RO and the receiver, respectively.

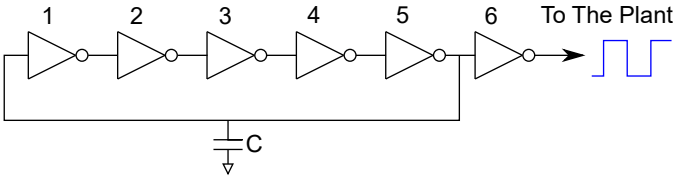

Fig. 2. Ring Oscillator schematics depiction. The purple and blue arrows represent the stainless steel needles used to inject and collect the signal into and from the plant. An external capacitance of 100 nF (C) has been connected between the first and fifth inverter to set the oscillating frequency at about 80 kHz.

The chosen signal frequency offered a good trade-off between the noisy behavior stem impedance has at low frequencies [9] and the distortion that higher frequency would introduce. Tests on the tobacco plant showed that for frequencies higher than 100 kHz, the signal collected at the receiver side presented distortion that would make the reading harder.

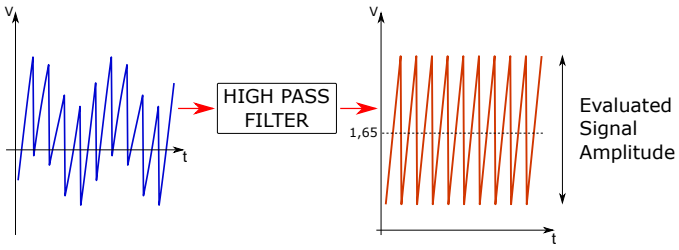

Fig. 3. The blue line represents the signal collected by the receiver from the plant, while the orange line is the signal fed to the threshold comparator. The collected signal is filtered, and its voltage is referenced to the receiver GND and a DC component equal to the midpoint of the common mode input range of the threshold comparator. Therefore, the high-pass filter output has a non-zero mean value.

The transmitter was powered by an LS14500 battery and an STLQ020 LDO voltage regulator, providing a stable supply voltage equal to 3.3 V. Keeping the supply voltage constant was a critical feature, as better detailed in section II-B. Since the RO output was rail-to-rail, the injected signal amplitude remained constant over time.

B. Receiver

The receiver's purposes are to collect the signal traveling through the plant (see figure 1), filter the noise, restore the digital behavior, and read its characteristics. Therefore, this device is composed of two blocks made of off-the-shelf components. The first block, responsible for noise filtering and restoring the digital behavior, comprises two sub-blocks: a passive first-order filter and an inverting threshold comparator. In figure 3, there are reported illustrations relative to the signal collected by the receiver and the one def to the threshold comparator. It was not possible to read these signals with an oscilloscope since its input impedance has the same order of magnitude as the resistance composing the filter. Therefore, connecting any probe would cause a shift in the filter cut-off frequency, resulting in poor noise filtering. The passive filter is a high-pass one. This sub-block has two duties. The first one is to filter the noise superimposed on the signal. Since the experiment was conducted indoors in Italy, the primary noise source was the power grid. Therefore, the filter cut-off frequency was set equal to 10 kHz, thus two orders of magnitude higher than the fundamental noise frequency (50 Hz). The second one was to restore the collected signal reference and set it equal to the receiver's GND. Moreover, it sets the signal's average value equal to the midpoint of the common mode input range of the inverting threshold comparator. The injected signal was referenced to the transmitter's GND. Therefore, the signal must be referenced to the receiver's GND to be appropriately managed by the following blocks. Once the signal was filtered, it was fed to an inverting threshold comparator made with a Texas Instruments TLV7011. This sub-block aimed to convert the analog signal from the filter into a square wave between the GND and the supply voltage. This was necessary since the second receiver block (detailed below) is a micro-controlling unit (MCU). The inverting threshold comparator had in its

feedback loop a digital potentiometer (AD 5272 made by Analog Devices) used to change the thresholds during the measurements dynamically. The circuit schematic is depicted in figure 4.

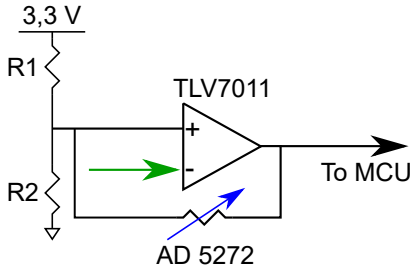

Fig. 4. Threshold comparator circuit schematics. The green arrow indicates where the signal coming from the high-pass filter is fed to the threshold comparator.

The threshold comparator usage and the measurement routine are detailed in the following. As already stated, this work's stem impedance monitoring methodology relies on a digital evaluation. The signal injected into the plant stem travels through it, and the receiver collects it at the bottom of the stem itself. Injected signal amplitude (V_{pp}) is controlled and set equal to $3.3\,\mathrm{V}$. A plant's stem is a resistive medium. Therefore, an electric signal traveling through it undergoes an attenuation. Thus, the collected signal amplitude is lower than the injected one. Signal amplitude attenuation is (in principle) directly proportional to the stem electrical impedance encountered by the signal while propagating. The measurement procedure evaluates the collected signal amplitude by dynamically modifying the voltage comparator thresholds. When the transmitter injects the signal, the receiver collects it, filters it, and sends it to the threshold comparator. This component is fed with an analog signal, and its output is a square wave fed to the MCU. While the comparator commutes, its thresholds are modified by the MCU. This happens since the AD5272 wiper position (thus the potentiometer resistance) can be set by an MCU through the I2C (inter-integrated circuit) communication protocol. Since the potentiometer is in the TLV7011 feedback loop, its resistance variations modify the comparator thresholds. The MCU enlarges the comparator hysteresis as long as it senses that the comparator output keeps commuting. Therefore, as long as a frequency equal to the injected signal one can be read by the MCU. Hysteresis enlargement is performed by reducing the digital potentiometer resistance. As soon as the comparator's hysteresis is too large to allow the commutation (thus, it overcomes the collected signal peak-to-peak amplitude), the MCU saves the hysteresis value and sends it to a laptop through UART (universal asynchronous receiver/transmitter) communication protocol. Hysteresis enlargement is performed step-wise. Therefore, the last hysteresis value allowing comparator commutation and the first one preventing it are sent to the laptop to perform the collected signal amplitude estimation. For simplicity, the peak-to-peak collected signal amplitude is equal to the average between the two hysteresis values transmitted to the laptop. At the end of this routine, the wiper position is reset, and the potentiometer resistance is set to the maximum. Thus, hysteresis is reset to its minimum. The measurement routine is described in figure 5.

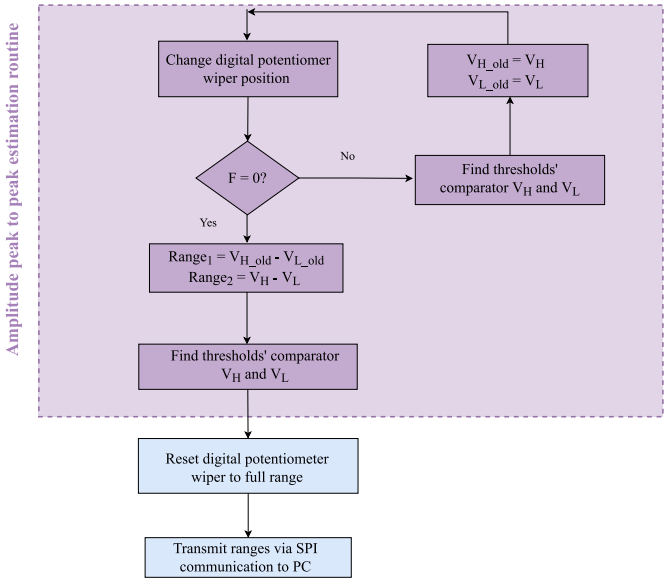

Fig. 5. Signal Amplitude estimation routine. The word "Range" stands for "hysteresis amplitude value". V_H and V_L are the two threshold value. $V_{H,old}$ and $V_{L,old}$ are the thresholds value evaluated at the previous step.

The second receiver block is the MCU mounted on the Nucleo-F401RE that runs a C script. As previously described, the MCU's duty was to dynamically enlarge the comparator hysteresis, collect data, and send them to the laptop where data analysis was performed. Since a laptop was involved in the process, measurement timing was performed manually. Thus, the signal injection was carried out by physically connecting the transmitter to the plant and the collection by starting the script responsible for changing the thresholds and collecting data running on the MCU.

III. Measurements and Results

Tests were performed on a single plant and lasted for approximately one month. Since this work presents a novel methodology that relies on human intervention and was not automatized, only a few measurements per day were performed. Stem electrical impedance was measured with our system and a bench instrument for validation. The instrument was an impedance meter, BK Precision 891, performing 4-probes impedance spectroscopy. The instrument was connected to the needles described in figure 1 used to connect the transmitter and the receiver to the plant. An impedance spectroscopy was performed after every signal attenuation evaluation made with the system described in this work. Only the impedance value evaluated at $80\,\mathrm{kHz}$ is considered and reported in the following plots. Moreover, since signal amplitude attenuation depends on the impedance modulus rather than its phase, the impedance phase will not be reported in the analysis. The comparison

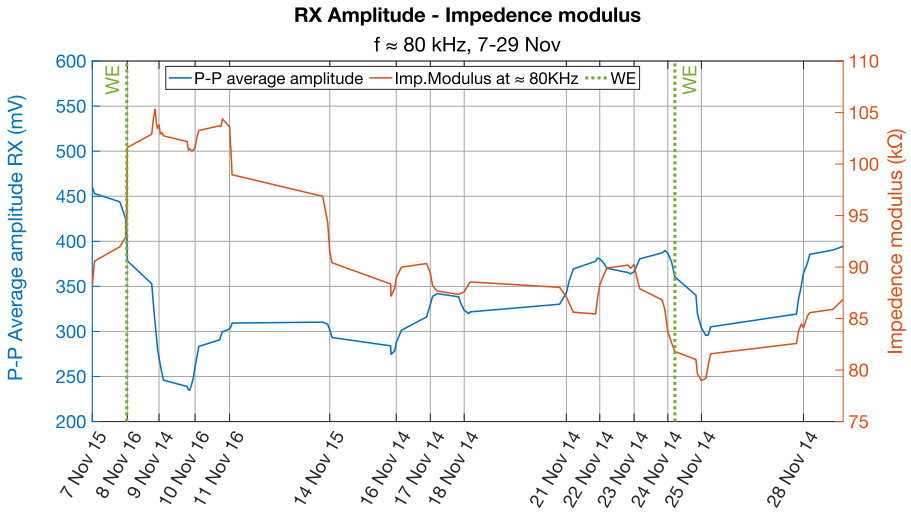

Fig. 6. The blue line refers to the peak-to-peak collected signal amplitude. The transmitter circuit design sets the injected one equal to 3.3 V. The red line refers to the stem impedance modulus evaluated at a frequency equal to 80 kHz. The green dashed vertical line highlights when a watering event occurred. On the horizontal axis are reported dates and hours at which the measurements took place.

between stem impedance modulus and signal attenuation is reported in figure 6.

Signal amplitude was evaluated as the average value between two hysteresis values, the last one able to trigger the comparator and the first too large to detect the input signal. Despite two watering events during the tests, stem impedance modulus' relative variations never exceeded 20%. This could be due to the choice of the inspecting frequency. High frequencies limit the stem impedance variation strength to external stimuli[6]. The second watering event (on November 24th) was performed when the plant was not particularly stressed. Its stem electrical impedance modulus was not as high as in the previous watering event. Therefore, both the impedance modulus and the signal attenuation do not show significant changes in their trends after this watering event. Nevertheless, it can be seen that stem impedance modulus and signal amplitude seem to be negatively correlated. In fact, after the first watering event, it can be seen that the stem electrical impedance modulus drops with a latency to the watering event. At the same time, the peak-to-peak signal amplitude has a dual behavior: it drops in correspondence to the impedance peak and rises later. Around the first watering event, it is visible that the signal amplitude is a good indicator of the stem impedance variation. Stem impedance modulus relative variation is around 10% (from 90 $k\Omega$ to 100 $k\Omega$) while the signal amplitude almost halved (from 450 mV to 240 mV). Data sets presented in this section underwent a *Pearson*'s correlation test. This test output is a value between -1 and +1, and it measures how strong the correlation between two data sets is. A negative correlation implies that two signals (represented by data sets) have a dual behavior: when one increases, the other decreases, and vice-versa. The positive correlation implies the opposite behavior. Correlation values between the collected signal amplitude and the measured stem impedance are reported in table I. The table diagonal entries are equal to 1 since they refer to the correlation that the data set has with itself, therefore, the auto-correlation. As figure 6 showed, the stem impedance modulus and the signal amplitude show a negative correlation as expected.

	Signal Amplitude	*Imp. Modulus*
Signal Amplitude	1	-0,54
Imp. Modulus	-0,54	1

TABLE I
Person'S CORRELATION COEFFICIENT EVALUATED FOR THE DATA SETS PRESENTED IN FIGURE6.

IV. Conclusions

This work presented a novel methodology to perform stem electrical impedance monitoring. This inspects the impedance of the whole stem and relies on the conductivity properties of any plant stem (or trunk). The system developed to perform measurements is completely composed of off-the-shelf devices. This feature dramatically reduces complexity, power, and costs with respect to the systems used up to now (i.e., bench instruments). Moreover, the measurement procedure relies on a fully digital approach that evaluates a signal's attenuation while traveling through the stem. This work did not implement measurement automation since it mainly aimed at validating the system. Nonetheless, given the system's low complexity, it would only require a few changes in the system design (such as substituting the MCU with one embedded with a wireless communication protocol) to be implemented. System overall dimensions and power consumption make the implementation possible in an actual field. In a future

perspective, the frequency of the injected signal could be used to modulate pieces of information. This way, a single signal can be analyzed to transmit multiple pieces of information.

ACKNOWLEDGMENT

Authors would like to thank Chiarillo Marta for her work on the system development. This study was carried out within the Agritech National Research Center and received funding from the European Union Next-GenerationEU (PIANO NAZIONALE DI RIPRESA E RESILIENZA (PNRR) – MISSIONE 4 COMPONENTE 2, INVESTIMENTO 1.4 – D.D. 1032 17/06/2022, CN00000022). This work was funded by the European Union - NextGenerationEU under the National Recovery and Resilience Plan (NRRP), Mission 04 Component 2 Investment 3.1 — Project Code: IR0000027 - CUP: B33C22000710006 - iENTRANCE@ENL: Infrastructure for Energy TRAnsition aNd Circular Economy @ EuroNanoLab. This manuscript reflects only the authors' views and opinions, neither the European Union nor the European Commission can be considered responsible for them.

REFERENCES

[1] H. Ritchie, L. Rodés-Guirao, E. Mathieu, *et al.*, "Population growth," *Our World in Data*, 2023, https://ourworldindata.org/population-growth.

[2] A. Burrell, J. Evans, and M. De Kauwe, "Anthropogenic climate change has driven over 5 million km2 of drylands towards desertification," *Nature communications*, vol. 11, no. 1, p. 3853, 2020.

[3] H. Ritchie, P. Rosado, and M. Roser, "Environmental impacts of food production," *Our World in Data*, 2022, https://ourworldindata.org/environmental-impacts-of-food.

[4] S. Tenzin, S. Siyang, T. Pobkrut, and T. Kerdcharoen, "Low cost weather station for climate-smart agriculture," in *2017 9th international conference on knowledge and smart technology (KST)*, IEEE, 2017, pp. 172–177.

[5] T. Kasama, T. Koide, W. P. Bula, Y. Yaji, Y. Endo, and R. Miyake, "Low cost and robust field-deployable environmental sensor for smart agriculture," in *2019 2nd International Symposium on Devices, Circuits and Systems (ISDCS)*, IEEE, 2019, pp. 1–4.

[6] U. Garlando, S. Calvo, M. Barezzi, A. Sanginario, P. M. Ros, and D. Demarchi, "Ask the plants directly: Understanding plant needs using electrical impedance measurements," *Computers and Electronics in Agriculture*, vol. 193, p. 106 707, 2022.

[7] V. Palazzari, P. Mezzanotte, F. Alimenti, F. Fratini, G. Orecchini, and L. Roselli, "Leaf compatible "eco-friendly" temperature sensor clip for high density monitoring wireless networks," *Wireless Power Transfer*, vol. 4, no. 1, pp. 55–60, 2017.

[8] U. Garlando, L. Bar-On, P. M. Ros, *et al.*, "Towards optimal green plant irrigation: Watering and body electrical impedance," in *2020 IEEE International Symposium on Circuits and Systems (ISCAS)*, IEEE, 2020, pp. 1–5.

[9] U. Garlando, L. Bar-On, P. M. Ros, *et al.*, "Analysis of in vivo plant stem impedance variations in relation with external conditions daily cycle," in *2021 IEEE International Symposium on Circuits and Systems (ISCAS)*, IEEE, 2021, pp. 1–5.

[10] M. Barezzi, F. Cum, U. Garlando, M. Martina, and D. Demarchi, "On the impact of the stem electrical impedance in neural network algorithms for plant monitoring applications," in *2022 IEEE Workshop on Metrology for Agriculture and Forestry (MetroAgriFor)*, 2022, pp. 131–135. DOI: 10.1109/MetroAgriFor55389.2022.9965011.

[11] F. Cum, S. Calvo, D. Demarchi, and U. Garlando, "Machine learning models comparison for water stress detection based on stem electrical impedance measurements," in *2023 IEEE Conference on AgriFood Electronics (CAFE)*, 2023, pp. 108–112. DOI: 10.1109/CAFE58535.2023.10291805.

[12] J. Yang, K. Liu, Z. Wang, Y. Du, and J. Zhang, "Water-saving and high-yielding irrigation for lowland rice by controlling limiting values of soil water potential," *Journal of Integrative Plant Biology*, vol. 49, no. 10, pp. 1445–1454, 2007.

[13] P. Dasgupta, B. S. Das, and S. K. Sen, "Soil water potential and recoverable water stress in drought tolerant and susceptible rice varieties," *Agricultural Water Management*, vol. 152, pp. 110–118, 2015.

[14] P. Ibba, A. Falco, A. Rivadeneyra, and P. Lugli, "Low-cost bio-impedance analysis system for the evaluation of fruit ripeness," in *2018 IEEE SENSORS*, 2018, pp. 1–4. DOI: 10.1109/ICSENS.2018.8589541.

[15] P. Ibba, A. Falco, B. D. Abera, G. Cantarella, L. Petti, and P. Lugli, "Bio-impedance and circuit parameters: An analysis for tracking fruit ripening," *Postharvest Biology and Technology*, vol. 159, p. 110 978, 2020.

[16] P. M. Ros, E. Macrelli, A. Sanginario, Y. Shacham-Diamand, and D. Demarchi, "Electronic system for signal transmission inside green plant body," in *2019 IEEE International Symposium on Circuits and Systems (ISCAS)*, IEEE, 2019, pp. 1–5.

[17] U. Garlando, S. Calvo, M. Barezzi, A. Sanginario, P. M. Ros, and D. Demarchi, "A "plant-wearable system" for its health monitoring by intra-and interplant communication," *IEEE Transactions on AgriFood Electronics*, 2023.

[18] S. Calvo, M. Barezzi, D. Demarchi, and U. Garlando, "In-vivo proximal monitoring system for plant water stress and biological activity based on stem electrical impedance," in *2023 9th International Workshop on Advances in Sensors and Interfaces (IWASI)*, IEEE, 2023, pp. 80–85.